IEEE Access
Multidisciplinary ⋮ Rapid Review ⋮ Open Access Journal

Received 26 April 2024, accepted 17 May 2024, date of publication 21 May 2024, date of current version 4 June 2024.

Digital Object Identifier 10.1109/ACCESS.2024.3403520

RESEARCH ARTICLE

An Improved Normalized Difference Vegetation Index (NDVI) Estimation Using Grounded Dino and Segment Anything Model for Plant Health Classification

ANANTHAKRISHNAN BALASUNDARAM[1,2], (Member, IEEE), ALABHYA SHARMA[2], SWAATHY KUMARAVELAN[2], AYESHA SHAIK[1,2], (Member, IEEE), AND MUTHU SUBASH KAVITHA[3]

[1]Centre for Cyber Physical Systems, Vellore Institute of Technology (VIT), Chennai 600127, India
[2]School of Computer Science and Engineering, Vellore Institute of Technology (VIT), Chennai 600127, India
[3]School of Information and Data Sciences, Nagasaki University, Nagasaki 852-8521, Japan

Corresponding author: Ananthakrishnan Balasundaram (balasundaram.a@vit.ac.in)

ABSTRACT Ensuring sustainable and profitable agriculture is critical for addressing global food security challenges. This has resulted in the need for automation in plant health identification. However, this objective is hampered by the lack of efficient image-processing methods and the need for extensive datasets for training deep learning models for plant disease diagnosis. To overcome the need for extensive training data, the proposed Localized Normalized Difference Vegetation Index (LNDVI) uses zero-shot plant detection models such as Grounded Dino and state-of-the-art methods for image segmentation such as Segment Anything Model (SAM) are leveraged. This also expands the capabilities of the system to diagnose plant health beyond known plant species available as part of training set. The proposed system uses synthetic Normalized Difference Vegetation Index (NDVI) to estimate the chlorophyll content of the plant through RGB images alone instead of using the combination of RGB and near Infra-red (nIR) bands used in contemporary works. Since NDVI value is greatly affected by the amount of light present while the image is captured, we also present an irradiation estimation metric that uses CIE XYZ (Tristimulus values), Hue, Saturation and Value (HSV) and CIE LAB color spaces as well as correlated color temperatures, which automatically normalizes the NDVI threshold for health classification of the image, enabling a more precise analysis of plant health. Using the Grounding Dino provided an accuracy of 99.994% in terms of detecting plants from the phenotyping dataset. The segmentation of plant region in images is reported using Intersection over Union (IoU). While using the Segment Anything Model (SAM), an average accuracy of 95.884% was obtained for clustered plants while the average accuracy was even better at 97.031% for individual plants. Significant differences were observed for plant health classification while using Localized Normalized Difference Vegetation Index (LNDVI) approach when compared to NDVI.

INDEX TERMS Agriculture, computer vision, Grounded Dino, NDVI, plant health, SAM.

I. INTRODUCTION

The 2022 Revision of World Population Prospects by the United Nations Secretariat estimates that the world population will cross 9 billion by 2037 [3]. With more people to feed, ensuring everyone has access to enough food is of utmost importance. This concept is known as food security [4], which aims to bridge the gap between the demand and supply of food. But despite the growing population, global food security has not improved. The Global Food Security Index for 2022 [5] reveals that overall food security in the world has remained stagnant

The associate editor coordinating the review of this manuscript and approving it for publication was Zhenhua Guo.

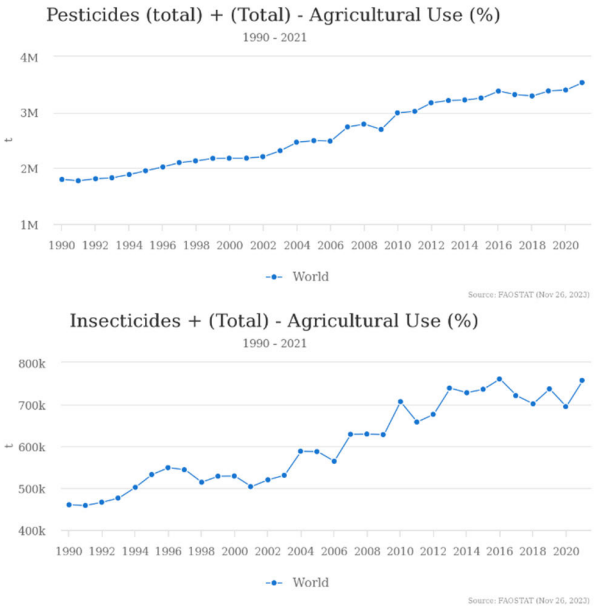

FIGURE 1. Visualization of world Pesticides and Insecticide usage from 1990-2020 [41].

compared to the 6% increase observed between 2012 and 2018.

Complex issues firmly rooted in the environment are to blame for the global challenge of feeding the expanding population and ensuring food security. To overcome this, governments need to invest in research and development (R&D) to ensure sustainability in the long term. By focusing on innovations that benefit farmers, we can not only increase productivity but also improve overall well-being, such as by reducing poverty.

Climate change and excessive farming practices contribute to crop failures. According to FAO [6], in 2021 alone, approximately 3.5 million metric tons of pesticides and 750 thousand metric tons of insecticides were used globally to combat diseases and pests. This excessive use of chemicals has also led to lower soil fertility. Figure 1 shows the year-wise trend observed in usage of pesticides and insecticides. By addressing these environmental challenges and promoting sustainable agriculture, we can work towards ensuring a stable food supply, protecting the environment, and improving the livelihoods of farmers and communities worldwide.

There are several shortcomings in the present system for addressing issues of agricultural productivity and disease detection. One major problem is the lack of funding and expertise needed to put effective solutions into practice. This hinders the adoption of helpful technologies in agriculture. Another issue is that existing classification models need to be trained separately for each plant type. This means that creating a large-scale dataset with accurate annotations for all plant types becomes a time-consuming and resource-intensive task. It would be more efficient to develop compute-effective deep learning solutions that can handle different plant types effectively, eliminating the need for separate training for each type. To overcome this, the development of large-scale, cost-effective solutions that can handle various plant types effectively is required.

Precision Agriculture is the application of advanced technologies that use a data-analytics-based approach to increase agricultural productivity. An important aspect of precision agriculture is the estimation of chlorophyll content in plants to determine their health status. Chlorophyll is a plant pigment that plays an essential role in photosynthesis, the process by which plants convert sunlight into energy. Various non-destructive methods, such as chlorophyll meters and hyper spectral imaging, are utilized to estimate chlorophyll content in leaves. These techniques analyze the absorption and reflection of light at specific wavelengths to derive chlorophyll levels. By measuring the chlorophyll content, farmers and scientists can understand the health status of a plant for timely intervention in cases of pests and diseases. Plant health estimation in precision agriculture not only helps optimize resource utilization but also promotes sustainable farming practices, reduces chemical inputs, and increases overall crop productivity.

The acquired data from specialised sensors, such as multispectral or hyperspectral cameras, is also used in remote sensing to evaluate the health and density of vegetation. These sensors are intended to measure the vegetation's reflectance in the near-infrared (NIR) and red (visible) regions of the electromagnetic spectrum. The Normalised Difference Vegetation Index (NDVI), also known as the ''greenness index'', is an indicator of chlorophyll content present in the plant. There are several spectral vegetation indices like NDVI, such as Normalised Difference Red Edge (NDRE), Green Normalised Difference Vegetation (GNDVI), etc. NDVI makes use of the near-infrared (NIR) and red bands of the electromagnetic spectrum, while GNDVI uses the NIR and green bands. NDRE detects changes in chlorophyll content and is used in later stages of the crop compared to NDVI.

Plant diseases and pests are one of the biggest obstacles to improving agricultural productivity. And hence the need for technological solutions that can automate plant health surveillance effectively. But such surveillance using visual features is challenging, not only due to morphological features but also lighting conditions. And given the lack of diverse datasets to train deep learning models effectively. Our work is focused on developing a farmer-centric system that does not require expensive sensors and can practically be applied for surveying any type of crop.

The primary objective of our system is to identify various plants in an image and accurately delineate their boundaries. Subsequently, we aim to apply brightness and contrast normalizations to the image, followed by the computation of a synthetic NDVI (Normalized Difference Vegetation Index). This process will generate color maps specifically tailored to the identified plant area within the image. Our system will then compare this Localized NDVI estimate with the RGB-based NDVI estimate (Synthetic NDVI) to validate this method. The final step involves classifying plant health by

comparing the mean NDVI values of plant areas to predefined thresholds. We aim to address these concerns by employing zero-shot detection and segmentation methods to evaluate their health status. For the purpose of this paper, our proposed system will henceforth be referred to as the Localized Normalized Difference Vegetation Index (LNDVI).

This research seeks to address several key questions related to plant detection, segmentation, and health classification using advanced techniques. The questions include the utilization of zero-shot techniques for plant detection and segmentation, enhancement of synthetic NDVI for accurate estimates without the use of nIR images, establishment of an irradiation estimation metric by combining various color spaces with correlated color temperatures, development of a Localized NDVI (LNDVI) to move away from data-driven approaches, and improvement of plant health classification using the LNDVI approach compared to traditional NDVI methods without the need for specialized nIR sensors. The scope of this research includes the following key deliverables and advancements:

- Utilization of zero-shot techniques for plant detection and segmentation to enable localisation.
- Enhancement of synthetic NDVI to get accurate NDVI estimates without utilizing nIR images.
- Establishment of an irradiation estimation metric combining CIE XYZ, HSV, and CIE LAB colour spaces with correlated colour temperatures to account for image brightness while normalizing NDVI thresholds.
- Development of LNDVI to move on from data-driven approaches for plant health identification.
- Significant improvement in plant health classification using the LNDVI approach compared to traditional NDVI methods without utilizing specialised nIR sensors.

II. RELATED WORKS

This section discusses the contemporary work done over the past decade or so related to the research's scope. Active research has been conducted on the application of Image Processing Techniques (IPT) and Machine Learning Algorithms (MLA) to extend the applications of Computer Vision in plant health detection [42]. Ngugi et al. [7], have provided a comprehensive review of recent plant disease recognition research utilizing image processing techniques. Harakannanavar et al. [8] proposed an approach that uses computer vision techniques like Histogram Equalization to improve image quality, segmenting the leaf samples using contour tracing, and different feature extractors such as wavelet transformations, principal component analysis, etc. These were then classified using SVM, K-NN, and CNN models, achieving high accuracy in identifying tomato disorders. Such shallow classifiers make the captured image go through processing and segmentation before feature extraction to eventually classify them. According to reports, deep learning techniques outperform shallow classifiers trained with manually extracted features.

In approaches that include deep learning, researchers focus on deep neural networks for classification, detection, and segmentation purposes. After evaluating ten cutting-edge CNN models [43], it was determined that DenseNet201, ResNet-101, and Inceptionv3 CNN architectures are the most appropriate models for desktop computers, whereas ShuffleNet and SqueezeNet are the most appropriate architectures for mobile and embedded applications. Liu et al. [9] outlined the works on disease detection using deep learning in recent years. Since they are limited to controlled environments and specific plant disease images, their results may not be applicable to different conditions or other plant diseases. Hence, it is important to note that a high recognition rate in one trial is not universal. A major challenge in training deep neural network-based systems for plant disease recognition is the scarcity of exhaustive, well-annotated datasets that cover a wide range of variations. Currently, the Plant Village Dataset [10], the Sunflower Dataset [11], and the Plant Phenotyping Dataset [12] are some of the widely used datasets. The plant village dataset has 61,486 images spanning 39 different classes of plant leaves. The sunflower dataset contains RGB, NIR images and ground truth segmentation of plants/weeds taken using a 4-channel multi-spectral camera. The Plant Phenotyping dataset has plants of tobacco or Arabidopsis with ground truth segmentations and further annotations and metadata.

To overcome the limitations of data availability, transfer learning is an effective approach. Transfer learning involves using pre-trained models and adapting them to new tasks, such as plant disease recognition. This technique leverages the knowledge learned from large-scale datasets and helps in training convolutional neural network (CNN) classifiers for other use cases easily. Chen et al. [13], proposed a novel deep learning architecture called INC-VGGN to identify plant disease images. They combined a pre-trained network called VGGNet with special modules called Inception modules. This system achieved an accuracy of 91.83% in identifying plant diseases using a public dataset. Even when the images had complex backgrounds, their approach had an average accuracy of 92.00% for identifying diseases in rice plants. In another study, Binnar et al. [14], evaluated four deep learning models, AlexNet, simple sequential model, MobileNet, and Inception-v3 to detect disease in leaves using the Plant Village dataset for training and testing. They concluded that the MobileNet model worked well with the dataset, achieving high training and validation accuracy of 99.07% and 97.52%, respectively. Eunice et al. [15], had concentrated on tweaking the hyperparameters of pre-trained models, such as DenseNet-121, ResNet-50, VGG-16, and Inception-v4 and training them on the popular Plant Village dataset. Their experiments showed that DenseNet-121 was particularly effective when there was a need to include a new plant disease in the model. This model had fewer parameters to train, making it easier to update with new information. The model achieved an impressive classification accuracy of 99.81% and an F1 score of 99.8%.

In [16], the performance of the EfficientNet architecture is compared with other popular deep learning models such as AlexNet, ResNet50, VGG16 and Inception V3. All the models were trained using transfer learning on both original and augmented versions of the Plant Village dataset. The results were evaluated using a separate test dataset, and it was found that the B5 and B4 models of EfficientNet had the highest validation scores compared to the other models. Whereas Gehlot et al. [17], proposed the EffiNet-TS, a model that not only classifies the plant disease but also a visualization of important symptoms by displaying the key features for categorizing that specific disease. The architecture based on EfficientNetV2 comprises the EffiNet-Teacher and EffiNet-Student classifiers and Decoder trained on the Plant Village dataset. By modifying the architecture of Teacher and student blocks with EfficientNetV2S and adding a DscDF (Dual skip connection deconv fusion) block in the decoder network they were able to solve overfitting concerns seen by ResTS with an F1 score of 0.989, Accuracy of 0.990 and Validation Loss of 0.045.

Segmentation of images has also shown improvements in accuracy for plant disease detection. Sharma et al. [18], had used segmented data to train the models. By using the S-CNN model trained on segmented images, they were able to improve performance by more than twofold. The proposed system by Haridasan et al. [19], utilised pre-processing and segmentation techniques along with support vector machine (SVM) classifiers and CNNs to recognize and classify specific types of paddy diseases. Their system achieved a high validation accuracy. While Kaya et al. [20], proposed a deep-learning solution for plant disease detection by incorporating RGB and segmented images. The DenseNet-based architecture was evaluated on the PlantVillage dataset and achieved an average accuracy of 98.17%.

Making spectral imaging systems more accessible, affordable, and user-friendly, benefits precision agriculture greatly. Stamford et al. [21] developed a low-cost NDVI imaging system based on Raspberry Pi and compared it to a costly camera, the Micasense RedEdge. They found that the low-cost system produced comparable NDVI values, showing that it's possible to achieve good results at a fraction of the cost. There has also been works that have trained machine learning models on such multispectral image datasets such as, Puteh et al. [22], who captured images of chili plants using two types of cameras (IR and No IR) to create their dataset. They used the NDVI index to extract features and trained models like Neural Networks, Naïve Bayes, and Logistic Regression to classify the plants. The Neural Network model had the highest accuracy in classifying plant health. Sahin et al. [23], developed a model to detect weeds and crops using a U-Net model with a ResNet50 architecture. They calculated NDVI images from a dataset of multispectral images and used a bilateral filter to obtain filtered Near-Infrared (NIR) images. By combining Green, Filtered-NIR, and NDVI channels as input to the model, they achieved good results in detecting weeds and crops.

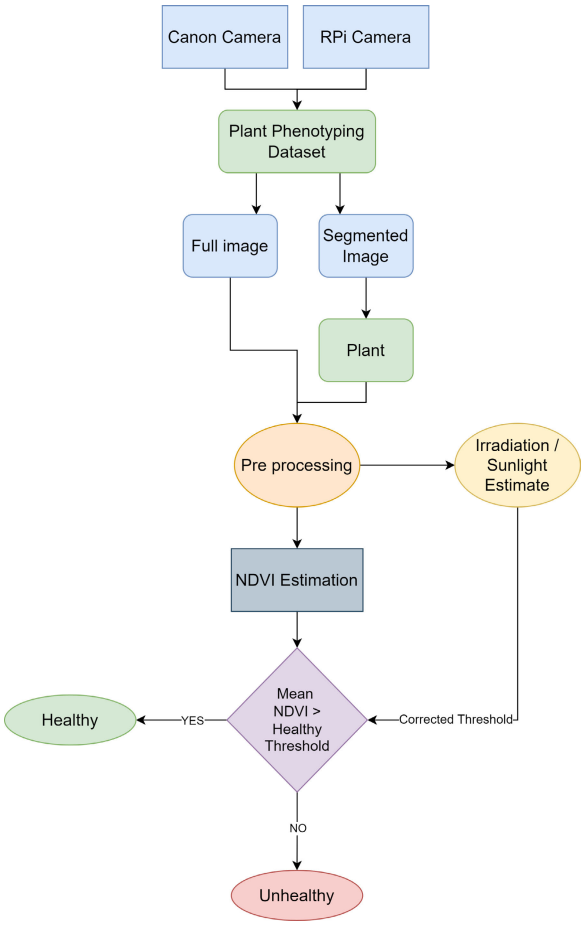

FIGURE 2. Workflow of the proposed system.

Generating an NDVI (Normalized Difference Vegetation Index) map typically requires a costly multispectral sensor. However, most unmanned aerial vehicles (UAVs) are equipped with affordable RGB cameras. To address this issue, Costa et al. [24] developed a genetic algorithm that calculates NDVI values from RGB maps from any RGB camera. The predicted NDVI values matched up to the values measured by multispectral cameras in different crops. It achieved a Mean Percentage Error (MPE) of 6.89% and a Mean Absolute Error (MAE) of 0.052. In [25], Yue et al. proposed a method to assess chlorophyll content and fractional cover using a Polar Coordinate Method (PCM) combined with the NDVI and Visible and Near-Infrared Angle Index (VNAI). This approach helps understand the differences in vegetation canopy and is referred to as VNAI-NDVI-space. Other indices include NDSI (soil salinity index) and MSAVI indices which are used for faster detection of problems with plant development, whereas the NDVI and NDRE (indicating chlorophyll activity in plants) are used at later stages of their development as suggested by Voitil et al. [26]. They emphasised the importance of agronomic surveys and yield maps to fully assess the feasibility of these indices. Plant-machine bio-interfaces such as Lu et al. 's research [27] and Wu et al. [28] help us develop special tools for precision agriculture.

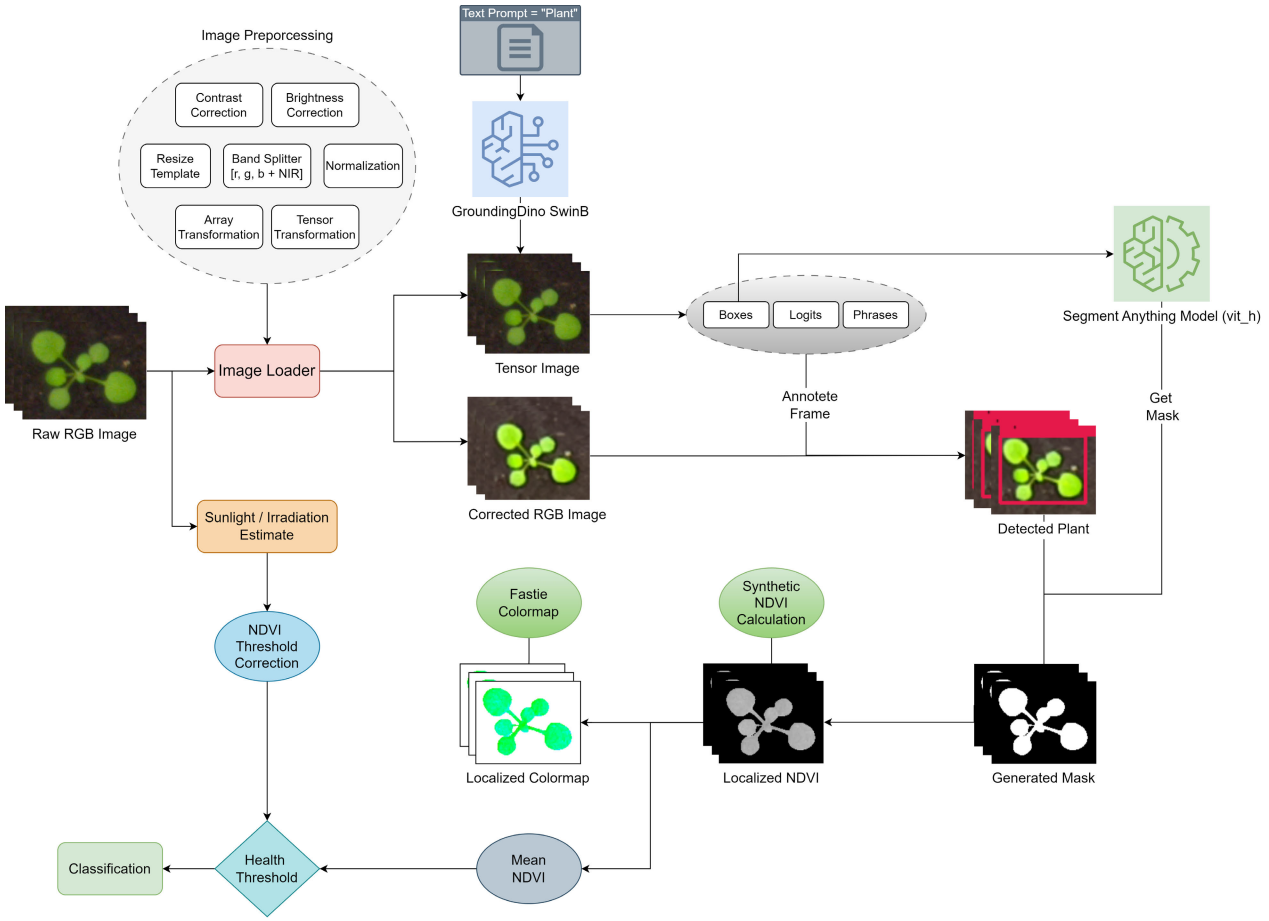

FIGURE 3. Components of the proposed Localised Normalised Difference Vegetation Index model for each image.

III. PROPOSED SYSTEM

The purpose of this research is to develop an improved method to identify diseased part of a plant using synthetic Normalised Difference Vegetation Index (NDVI) calculation that enables the accurate categorization of individual plant health status based on RGB images acquired by any camera under varying lighting conditions. Figure 2 shows the workflow of the proposed research. It uses the Plant Phenotyping dataset [12] to get NDVI values for both normal and segmented methods. Then, threshold corrections based on the brightness of the image from the irradiation estimate are used to sort the values into healthy and unhealthy groups. The outputs of this procedure are then subjected to stringent comparisons to ensure the validity and effectiveness of the proposed system.

Experiments using LNDVI (Localised Normalised Difference Vegetation Index) will utilise two types of image datasets in this research, namely, Plant and Tray image datasets, where Plant dataset contains images of single plants and tray dataset contains multiple plants. These images are subjected to Irradiation (sunlight) estimation, plant detection, and segmentation. The images are then contrasted, and the specific regions containing plants are masked out for NDVI calculation as shown in Figure 3.

TABLE 1. Hyperparameter for grounded sam.

Item	Value
Optimizer	AdamW
Activation	GELU
Text Encoders (Dino)	DINO, SAM
Image Embeddings	256 X 64 X 64
1 X 1 Convolution	256 Channels
3 X 3 Convolution	256 Channels
Feature Dimension	2048 Layers
Hidden Feature Dimension	256 Layers
Encoders	6 Layers
Decoders	6 Layers

The proposed system consists of four blocks.

- Plant detection and segmentation
- NDVI estimation
- Brightness estimation
- Health Classification

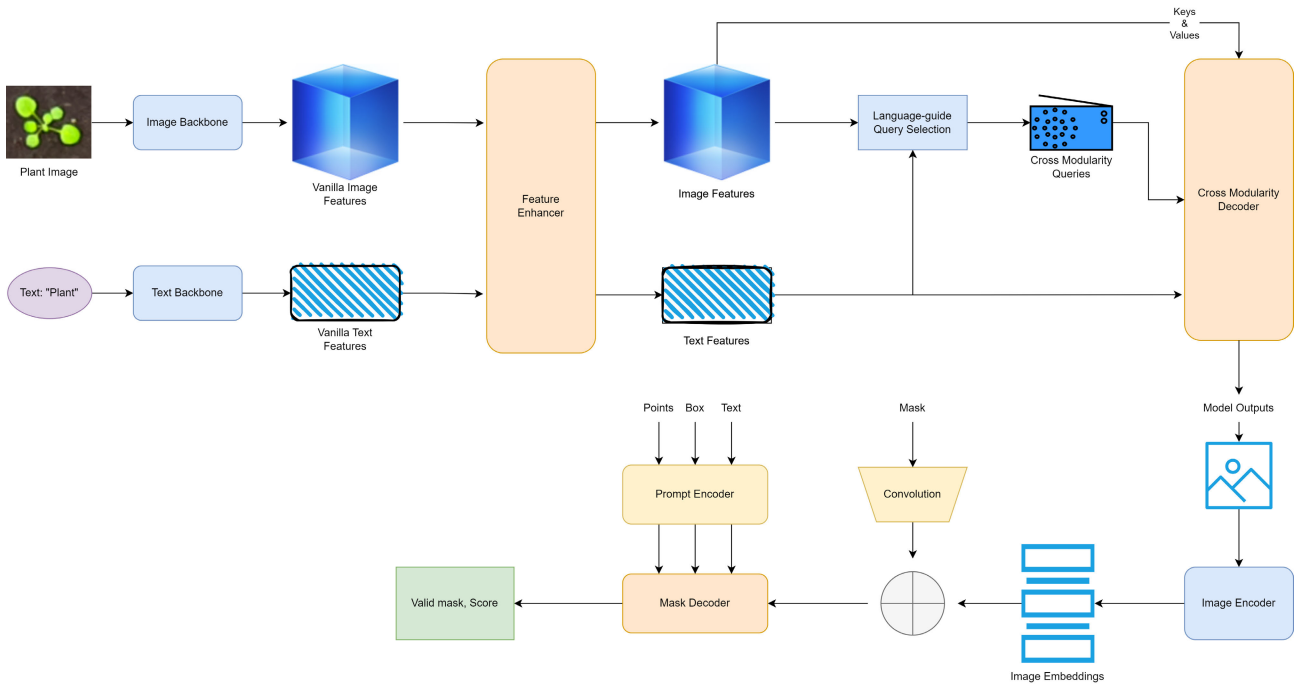

FIGURE 4. Architecture diagram for Grounded Dino and SAM.

A. PLANT DETECTION AND SEGMENTATION

To achieve zero-shot detection and segmentation, we make use of two SOTA technologies, namely the Grounded Dino and Segment Anything Model. The architecture of this model is shown in Figure 4 while using the hyperparameters of the model are mentioned in Table 1.

1) GROUNDED DINO

Object detection is an elementary task in computer vision. Traditional methods typically rely on classical convolution-based object detection that generates anchors (reference boxes) and applies non-maximum suppression to select the best matches. In contrast, Transformer-based object detection models, such as DETR (DEtection TRansformer) [29], leverage the power of Transformers to understand the contextual relationships between different image regions. In continuation of DETR, Zhang et al. and others propose DINO (DETR with Improved deNoising anchor box) [30]. DINO is a variant of DETR consisting of various components, such as a backbone network, a Transformer encoder and decoder, and prediction heads. DINO's impressive scalability can be traced to the contrastive denoising training to prevent duplicate outputs, the dynamic anchor box formulation of queries, and the look-forward twice scheme to correct the updated parameters with gradients from successive layers.

The concept of zero-shot object detection revolves around using text prompts to identify previously unseen objects. These ''open-set detectors'' are developed by extending pre-existing closed-set detectors with language information. Since language models are also based on Transformers, using Transformer-based detectors, such as DINO is more convenient. Therefore, to achieve zero-shot detection, Liu et al. [1], propose Grounded DINO, which combines DINO with grounded pre-training.

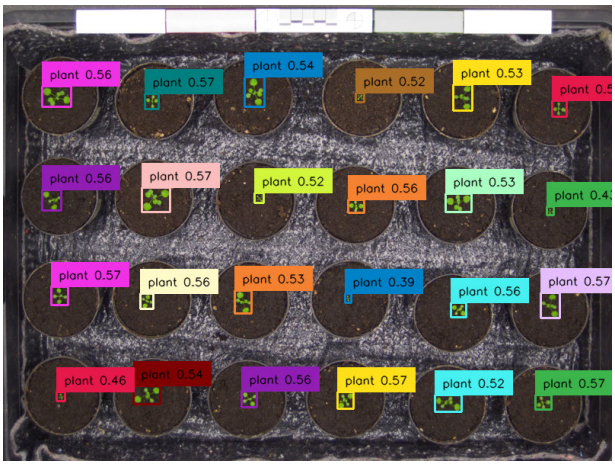

FIGURE 5. Plant detection using Grounded Dino.

To detect plants in an image, the image and the prompt ''Plant'' are provided as inputs to the model. Both inputs are subjected to feature extraction before being forwarded to the feature enhancer module for cross-modality feature fusion. A language-guided query selection selects the appropriate cross-modality queries from the image features, which are then fed to a decoder, which extracts the relevant features and updates itself. The output queries of the final decoder layer help to predict object boxes and extract the respective phrases, as shown in Figure 5. This deep fusion strategy is what

FIGURE 6. Plant segmentation using SAM.

leads to Grounding Dino's impressive zero-shot detection. However, Grounding DINO is not applicable to segmentation tasks, focusing primarily on object detection.

2) SEGMENT ANYTHING MODEL

Influenced by the advancements in zero-shot and few-shot learning techniques that utilise "prompting" methods, Kirillov et al. [2], introduce a promptable foundation model called SAM (Segment Anything Model) that is pre-trained for image segmentation. The model generates accurate segmentation masks based on various text prompts given, as shown in Figure 6 (For prompt "Plant").

SAM consists of three key elements: an image encoder, a flexible prompt encoder, and a rapid mask decoder. The Image encoder uses a pre-trained Vision Transformer (ViT) trained by MAE [31]. The prompt encoder utilizes an easily accessible text encoder from CLIP [32]. The mask decoder effectively maps the image embedding, the prompt embeddings, and an output token to generate the desired mask. In addition, a modified Transformer decoder block and a dynamic mask prediction head are incorporated into the design. The design of the model prioritizes efficiency by employing a modified Transformer decoder block and a dynamic mask prediction head. In addition, the model's runtime performance is exceptional, with the prompt encoder and mask decoder running locally on an Intel i7 CPU in approximately 50 milliseconds, enabling real-time interactive prompting of the SAM model.

B. NDVI ESTIMATION

A vegetation index (VI) is a spectral imaging technique that combines different bands of the electromagnetic spectrum to analyze and improve vegetation properties. For photosynthesis, green plants absorb photosynthetically active radiation (PAR) from the sun. This mechanism causes chlorophyll to absorb visible light (from 400 to 700 nm) with great intensity. However, they emit the same energy because the high photon energy at wavelengths beyond 700 nanometers makes it difficult to synthesize organic molecules, causing them to strongly reflect near-infrared light (from 700 to 1100 nm). This inverse relationship between red and near-infrared reflectance in healthy green vegetation is the foundation for numerous vegetation indices, allowing it to be used as a measure of a plant's photosynthetic capacity [33].

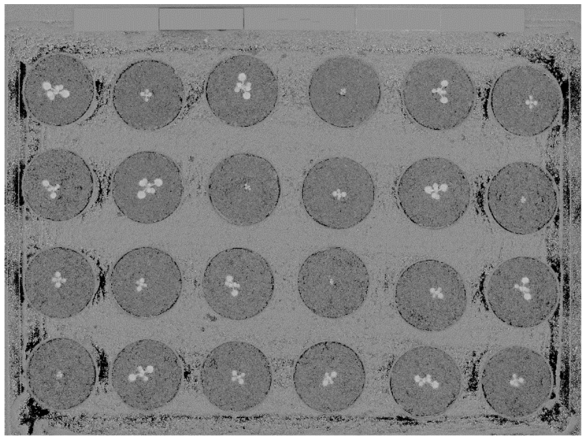

FIGURE 7. NDVI estimate of an image from Tray dataset.

Normalized Difference Vegetation Index (NDVI) is a commonly used index that is computed by dividing the difference between near-infrared (NIR) and red reflectance by their sum. Applying a convolution operation with a kernel, where image will be denoted as I, $I_{(i,j)}$ represent pixel at location (i, j) within the image matrix , I_{Red} and I_{NIR} denoting the Red and NIR channels of image respectively, we get (1).

$$NDVI_{i,j} = \frac{I_{NIR_{i,j}} - I_{Red_{i,j}}}{I_{NIR_{i,j}} + I_{Red_{i,j}}} \tag{1}$$

Rouse et al. [34] demonstrated a strong correlation between NDVI and grassland vegetation data, indicating its association with photosynthetic capacity and energy absorption in plant canopies. Gitelson et al. [35] proposed another index called VIgreen (Synthetic NDVI), that focuses on the contrast between green and red reflectance for monitoring wheat canopies. Applying a convolution operation over the Green channel instead of NIR in (1) gives us (2).

$$VIgreen_{i,j} = \frac{I_{Green_{i,j}} - I_{Red_{i,j}}}{I_{Green_{i,j}} + I_{Red_{i,j}}} \tag{2}$$

In addition to these indices, other combinations of reflectance values in the blue, red, green, and red edge bands are used to estimate vegetation fraction in different crops. These indices have shown greater validity in certain crops compared to the commonly used red/NIR indices. They leverage the subtle differences among the reflectance values in these bands to estimate vegetation health. By calculating these vegetation indices from the reflectance values of the corresponding bands in an RGB image, we assess the health and condition of plants. These indices provide valuable insights into the photosynthetic activity and energy absorption capabilities of vegetation, allowing for effective monitoring and analysis of vegetation health. Figure 7 and Figure 8 show the brightened and color mapped NDVI estimate respectively of the Image.

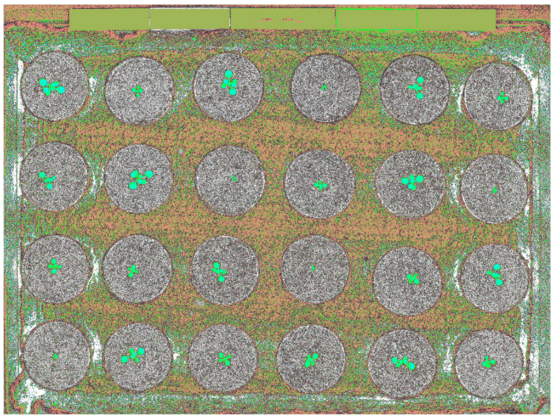

FIGURE 8. Colour mapped NDVI of an image from Tray dataset.

C. BRIGHTNESS ESTIMATION

The intensity of sunlight can vary throughout the day, and this variation impacts the reflectance properties of leaves, leading to fluctuations in the NDVI. To address this, we propose specific techniques to estimate the perceived brightness of an image. In color spaces like CIE XYZ (CIE 1931 color space), CIE LAB, and HSV (Hue, Saturation, Value), we can represent the full gamut of colors perceived by humans. In XYZ space, Y represents luminance, Z is similar to blue, and X is a mix of the three primary colors, red, green, and blue. While in the LAB L represents perceptual lightness and A, and B for the four primary colors red, green, blue and yellow. The L component captures the human perception of lightness, with 0 indicating black and 100 indicating white. On the other hand, the HSV color space describes colors based on their hue, saturation, and value (brightness) by arranging hues in a circular pattern and ranging from darker to lighter tones from bottom to top.

To estimate whether an image is predominantly dark or light, we compute the Normalized arithmetic means of the Y channel from XYZ space, the L channel from LAB space, and the V channel (brightness) from HSV space. Sunlight has a spectral distribution similar to that of a black-body radiator. Hence it has a correlated color temperature of 6500 K corresponding to the average daylight known as D65 [36]. This D65 illuminant represents the average midday light in Western and Northern Europe. As per CIE 1931 color space, the coordinates for this average daylight are x =0.31272 and y =0.32903 [37]. The point on the Planckian locus closest to the white point of the light source is calculated using MacAdam's (u,v) diagram [38], where u and v are calculated as shown below in (3) and (4).

$$u = \frac{4x}{12y - 2x + 3} \tag{3}$$

$$v = \frac{6y}{12y - 2x + 3} \tag{4}$$

The chromaticity coordinates (x, y) are calculated from the XYZ color space using (5) and (6).

$$x = \frac{X}{X + Y + Z} \tag{5}$$

$$y = \frac{Y}{X + Y + Z} \tag{6}$$

By comparing this white point of an image to that of the daylight illuminant, we can estimate its brightness level. Let the Image be denoted by I and its LAB, XYZ, HSV representations as $I_{LAB}, I_{XYZ}, I_{HSV}$ respectively. The channels L, Y, V channels can be represented as $I_{L,}, I_Y, I_V$ respectively. If there are N number of pixels in the image, we get the normalized mean of L, Y, V in (7).

$$M(L, Y, V) = \frac{1}{N} \sum_{i=1}^{N} (I_{L_i}, I_{Y_i}, I_{V_i}) \tag{7}$$

After getting the normalized mean for L, Y and V i.e., M_L, M_Y and M_V respectively, these values are compared to a threshold of 0.7. The result of that comparison is assigned to a respective Boolean flag. For UV, this flag is set based on D65 chromaticity coordinates represented in (8). Conjunction of these flags determines if the image is bright or not as depicted in (9).

$$flag_{UV} = (u, v) \approx (0.31272, 0.32903) \tag{8}$$

$$isBright = flag_L \wedge flag_Y \wedge flag_V \wedge flag_{UV} \tag{9}$$

D. HEALTH CLASSIFICATION

The values for NDVI range from −1 to 1. Negative values indicate water and non-vegetated objects, while vegetation falls between 0 to 1. Bare soil typically has values around 0.1. Plants have positive values ranging from 0.11 to 0.72 [39], the peak values for plants being 0.8 to 0.9 [21]. Considering this, NDVI values above 0.66 correspond to healthy plants, and values below 0.33 are classified as unhealthy. In dimly lit images, these values are adjusted to 0.45 and 0.15, accounting for the reduced brightness of green pixels. These adjustments help accommodate the varying illumination conditions and ensure an accurate interpretation of the NDVI values in the image.

IV. EXPERIMENTAL RESULTS

Our study utilizes a plant phenotyping dataset [12] consisting of 2 sets of images. The first set contains individual plant images [Plant] which has 165 RGB images captured using both Canon and RPi cameras along with a mask for plants. The second one contains Multiple plants in 1 image [Tray] which has 27 RGB images. Running the model on each image provided NDVI image, Mean NDVI value, brightness status, health status, Color Mapped NDVI image, Boxed plant detection image, Segmented image, LNDVI image, Color Mapped LNDVI image, mean LNDVI, brightness status and health status of each plant for every image in datasets. We evaluated the performance of each sub models through experiments performed in a python interface hosted on a Google Colab notebook powered by an L4 GPU [40]. These results are presented as follows:

A. OBJECT DETECTION

The results of our experiments demonstrate the effectiveness of the proposed methodology. In the analysis of both

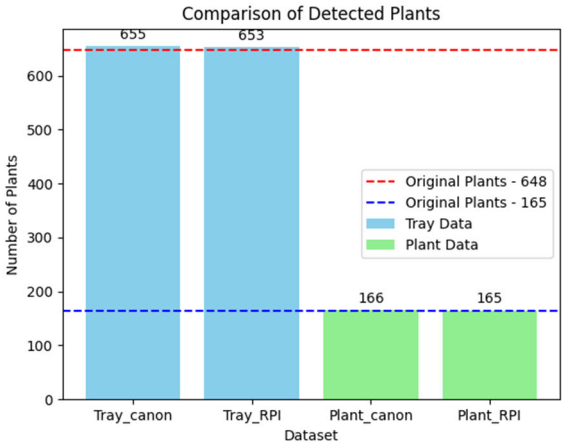

FIGURE 9. Comparison of values returned by Grounded Dino with the ground truth.

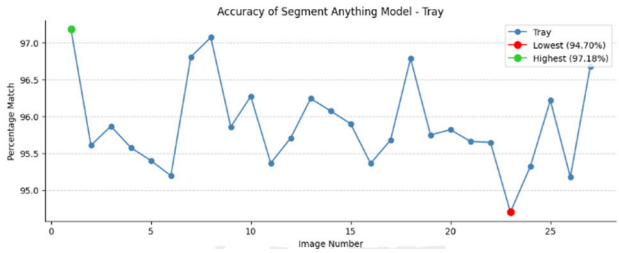

FIGURE 10. The percentage of area segmented by SAM matching the original image segments provided in Tray dataset with average mean accuracy of 95.884%.

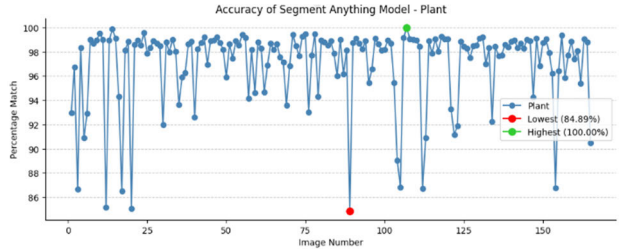

FIGURE 11. The percentage of area segmented by SAM matching the original image segments provided in Plant dataset with average mean accuracy of – 97.031%.

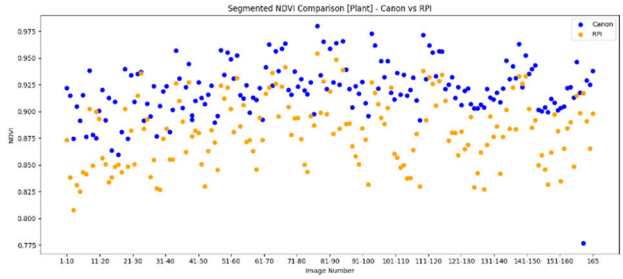

FIGURE 12. The LNDVI values of each plant in the Plant dataset for both Canon and RPi images are represented in different colors.

the Canon and RPi camera images for both the subsets showing an accuracy of 99.989% [Tray_canon], 99.992% [Tray_RPI], 99.994% [Plant_canon] and 100% [Plant_rpi] giving an average accuracy of 99.994% for plant detection using the GroundingDino python library as shown in Figure 9

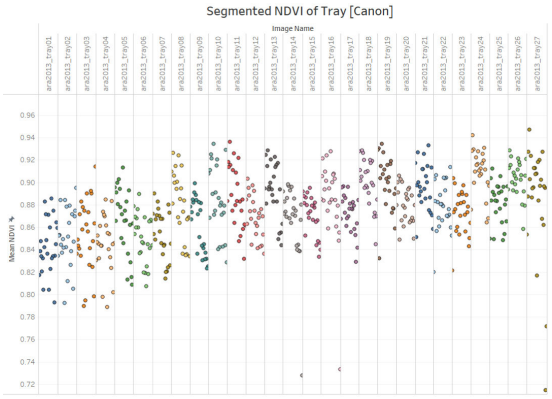

FIGURE 13. LNDVI pf each plant in the Tray dataset images taken with Canon camera. Circles in the same segment having same color represent planta from the same image.

(plotted using matplotlib). This accuracy was calculated by dividing the number of detected plants by the original number of plants.

B. PLANT SEGMENTATION

To evaluate the segmentation accuracy, we compared the image segments of plants generated by SAM (using segment anything python library) with the ground truth masks provided in the dataset [12] by using Intersection over Union (IoU) metric also known as Jaccard Index. The results revealed an impressive accuracy of up to 97.18%, with a lower limit of 94.7% for Tray and up to 100% with a lower limit of 84.89% for the Plant dataset, as shown in Figure 10 and 11 respectively. This suggests that SAM is capable of accurately delineating the boundaries of individual plants, thereby enabling precise analysis of plant-related characteristics.

These findings demonstrate the potential of combining SAM and Grounding Dino for accurate plant phenotyping and vegetation analysis. The integration of advanced computer vision techniques, such as SAM, allows for efficient and automated plant segmentation, saving significant time and effort in manual annotation.

C. COMPARISON BETWEEN SYNTHETIC NDVI AND LNDVI VALUES

To further investigate the performance of our approach, we compared the NDVI values of the segmented plants with the normal NDVI values of the entire image. The resulting charts, as seen in Figure 12, 13 and 14 (plotted in tableau), provide valuable insights into the vegetation health of the individual plants where each dot represents a plant. By analyzing the NDVI values, researchers can gain a deeper understanding of plant growth patterns, stress levels, and overall health.

When coupling LNDVI values with original values, a significant difference can be observed in Figure 15 and 16. This difference is subjected to various factors, such as the small size of plants, the lower density of vegetation, and the

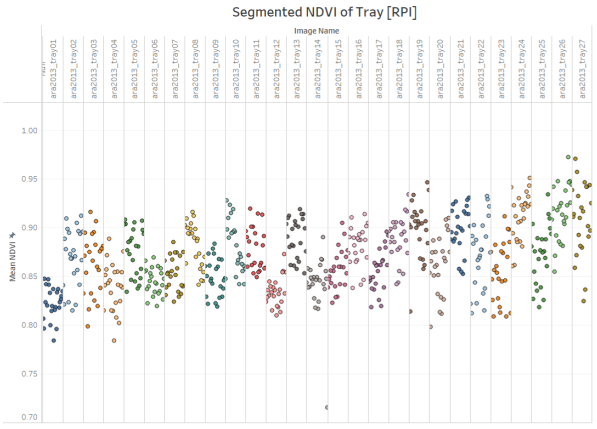

FIGURE 14. LNDVI pf each plant in the Tray dataset images taken with RPi camera. Circles in the same segment having the same color represent plants from the same image.

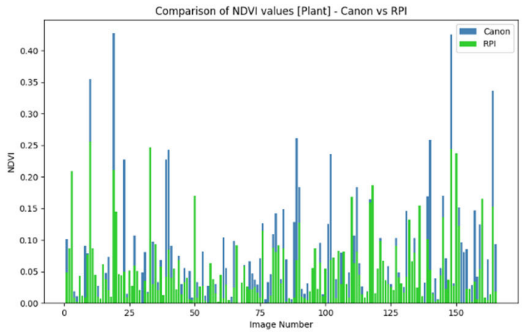

FIGURE 15. Synthetic NDVI values of RGB images from Plant dataset.

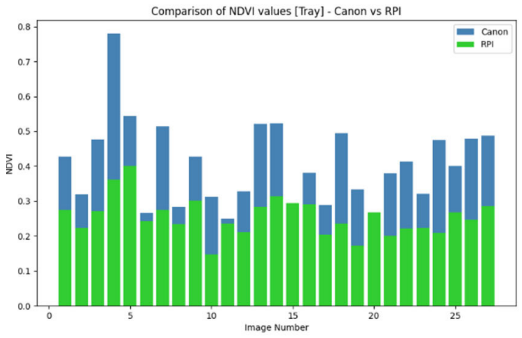

FIGURE 16. Synthetic NDVI values of RGB images from Tray dataset.

lighting conditions in the images. The variation of these values depending on the camera is also observed to be reduced.

D. HEALTH CLASSIFICATION

It is worth noting that the high accuracy achieved in our experiments is attributed to the quality of the dataset and the robustness of the applied methodologies. However, certain challenges and limitations may arise in real-world scenarios, such as varying lighting conditions, occlusions, or complex background elements. To account for lighting-based issues, inferences were extracted from LNDVI values using predefined threshold values [21] and corrected threshold values after checking for image brightness, as shown in Figure 17, 18, 19 and 20.

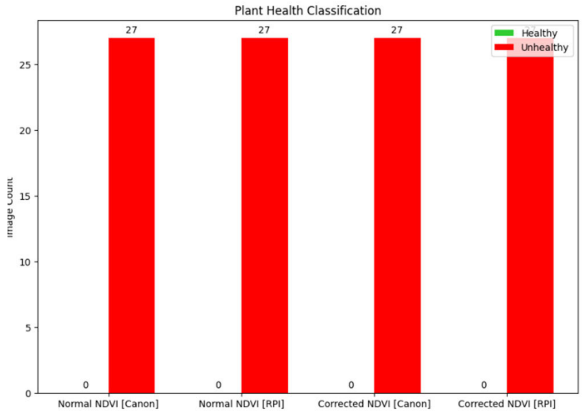

FIGURE 17. Results of plant health classification by using synthetic NDVI on Tray images.

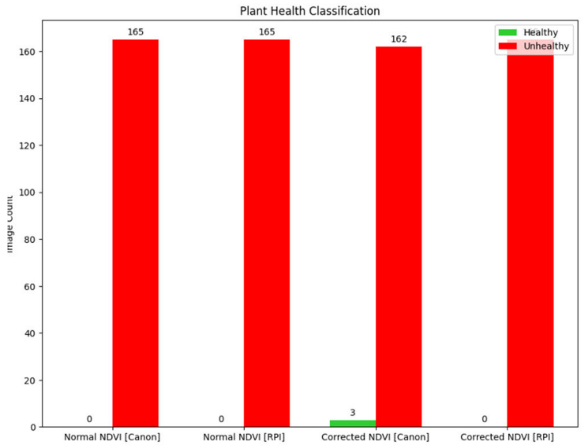

FIGURE 18. Results of plant health classification by using synthetic NDVI on individual Plant images

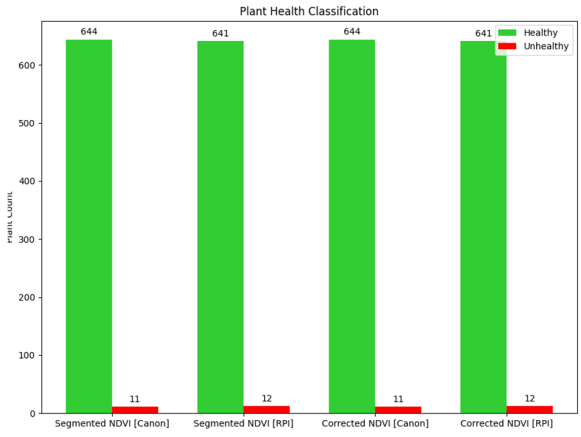

FIGURE 19. Results of plant health classification by using LNDVI on Tray images

V. EXPERIMENTAL RESULTS DISCUSSION

This discussion section aims to interpret the experimental results and provide insights into the metrics used and their implications for the proposed system. In this research, we developed the LNDVI (Localized Normalized Difference Vegetation Index) method, which leverages advanced computer vision techniques for plant detection and segmentation

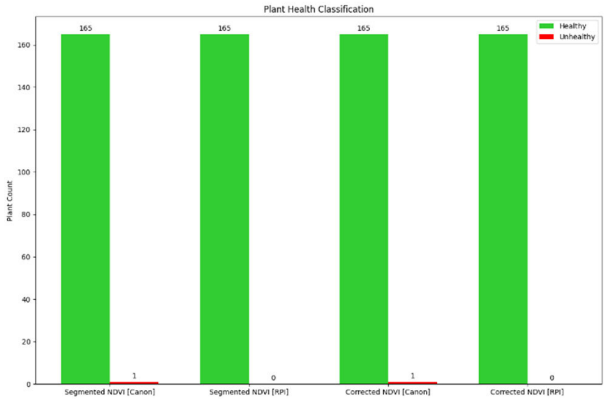

FIGURE 20. Results of plant health classification by using NDVI on individual Plant images

TABLE 2. Average accuracies of different models for health classification.

Model	Dataset	Average Accuracy in percentage
INC-VGGN (VGGNet + Inception modules) [13]	Public Dataset	91.83
AlexNet, Simple Sequential Model, MobileNet, Inception-v3 [14]	Plant Village Dataset	97.52
DenseNet-121, ResNet-50, VGG-16, Inception-v4 [15]	Plant Village Dataset	99.81
EffiNet-TS (EffiNet-Teacher, EffiNet-Student, Decoder) [17]	Plant Village Dataset	99.0
Normalized Difference Vegetation Index (NDVI)	Plant Phenotyping Dataset	45
Localized Normalized Difference Vegetation Index (LNDVI)	**Plant Phenotyping Dataset**	**99.7**

and combines it with brightness estimation to improve NDVI calculations. LDNVI was successful in classifying the health of individual plants, which NDVI has been observed to fail in. The results are then used for the health classification of individual plants based on their NDVI values. Further ground truth in the plant phenotyping dataset is required to account for the accuracy of LNDVI.

A. OBJECT DETECTION AND SEGMENTATION

The experimental results show that by combining Grounded DINO and SAM we can achieve remarkable accuracy in object detection and segmentation. Grounded DINO detects plants in both Canon and RPi camera images, yielding an average accuracy of 99.994%. SAM, on the other hand, achieves impressive segmentation accuracy, accurately tracing the boundaries of individual plants with a mean accuracy of up to 97.18% for Tray images and up to 100% for Plant images on Jaccard Index. This demonstrates the robustness of the proposed system in accurately identifying and segmenting plants, enabling precise analysis of plant-related characteristics.

B. NDVI AND LNDVI ESTIMATION

The NDVI is a widely used vegetation index that quantifies vegetation health. By comparing the NDVI values of the entire images with the calculated values using the proposed LNDVI method, we gain valuable insights into the health and growth patterns of individual plants. The LNDVI values help in mitigating issues related to varying lighting conditions. The analysis of LNDVI values reveals a significant difference between the values obtained using the proposed method and the traditional NDVI values calculated for the entire image. This difference is attributed to factors like vegetation density, and varying lighting conditions, which are effectively addressed by the LNDVI approach.

C. HEALTH CLASSIFICATION

Based on the NDVI and LNDVI values obtained, a health classification is performed for individual plants. The threshold values used for health classification are adjusted based on the brightness of the image, ensuring an accurate interpretation of plant health under varying lighting conditions. The health classification results indicate that the proposed LNDVI method provides more accurate results (an average accuracy of 99.7%) and robust assessment of plant health compared to traditional NDVI calculations (average accuracy of 45%) at a plant scale as shown in Table 2 alongside a comparison with supervised learning models. The LNDVI method is observed to reduce the variation in health classification results across different cameras, enhancing the generalizability of the proposed system.

VI. CONCLUSION

This research work successfully demonstrates the application of SAM and Grounding Dino in accurately detecting and segmenting individual plants from RGB images. The high average accuracy of 99.994% achieved in plant detection and average IoU of 96.457% achieved in segmentation, coupled with the insightful analysis of NDVI values, displays the capability of this methodology in classifying plant health by normalizing the NDVI health threshold based on image brightness. This has extended the application of NDVI from assessing vegetation density at remote sensing levels to a more grounded and generalized health metric for individual green plants where an average shift of 99.25% was observed due to localization on a plant level. This advancement eliminates the need for specialized near-infrared sensors, thereby increasing the efficiency of synthetic NDVI in precision agriculture and narrowing the gap between expensive multispectral cameras, such as the Parrot Sequoia and MicaSense Red Edge, and more accessible RGB cameras, including those in smartphones. The findings of this study contribute to the advancement of computer vision techniques in the field of agriculture and hold promise for improving agricultural

practices and environmental monitoring. LNDVI can set up the basis for modern-day plant health classification systems in precision farming to accurately identify affected plants among many. This approach will provide an in-depth analysis of a crop's lifecycle, which researchers can utilize to identify patterns in factors affecting plant growth and engineer ways to increase crop productivity to keep up with the increasing food demands of the ever-growing population of the world. Future research can focus on extending the proposed system to handle more challenging scenarios, such as partial occlusions and dense vegetation. Improvements can be made to enhance the robustness of the health classification process under varying illumination conditions and address potential issues related to noise and image artefacts.

ACKNOWLEDGMENT

The authors would like to thank VIT Chennai management for their support during this research work. Agriculture technology-related suggestions were given by Dr. Narender Kumar Sankhyan (HoD, Soil Science Department) and Ashish Dhiman (Home Sciences Department) of CSKHPKV Palampur, Himachal Pradesh.

REFERENCES

[1] S. Liu, Z. Zeng, T. Ren, F. Li, H. Zhang, J. Yang, C. Li, J. Yang, H. Su, J. Zhu, and L. Zhang, "Grounding DINO: Marrying DINO with grounded pre-training for open-set object detection," 2023, *arXiv:2303.05499*.

[2] A. Kirillov, E. Mintun, N. Ravi, H. Mao, C. Rolland, L. Gustafson, T. Xiao, S. Whitehead, A. C. Berg, W.-Y. Lo, P. Dollár, and R. Girshick, "Segment anything," 2023, *arXiv:2304.02643*.

[3] United Nations. (2022). *Population Division. Licensed Under Creative Commons License CC BY 3.0 IGO. United Nations, DESA Population Division, World Population Prospects 2022*. [Online]. Available: https://population.un.org/wpp/Graphs/DemographicProfiles/Line/900

[4] A. D. Tripathi, R. Mishra, K. K. Maurya, R. B. Singh, and D. W. Wilson, "Estimates for world population and global food availability for global health," in *The Role of Functional Food Security in Global Health*. USA: Academic, 2019, pp. 3–24, doi: 10.1016/B978-0-12-813148-0.00001-3.

[5] *Global Food Securities Index 2022*. Accessed: May 31, 2023. [Online]. Availabile: https://impact.economist.com/sustainability/project/food-security-index/

[6] Food and Agriculture Organization of the United Nations. (2018). *FAOSTAT Pesticides and Insecticides Use Dataset*. [Online]. Available: http://www.fao.org/faostat/en/#data/RP

[7] L. C. Ngugi, M. Abelwahab, and M. Abo-Zahhad, "Recent advances in image processing techniques for automated leaf pest and disease recognition – a review," *Inf. Process. Agricult.*, vol. 8, no. 1, pp. 27–51, Mar. 2021, doi: 10.1016/j.inpa.2020.04.004.

[8] S. S. Harakannanavar, J. M. Rudagi, V. I. Puranikmath, A. Siddiqua, and R. Pramodhini, "Plant leaf disease detection using computer vision and machine learning algorithms," *Global Transitions Proc.*, vol. 3, no. 1, pp. 305–310, Jun. 2022, doi: 10.1016/j.gltp.2022.03.016.

[9] J. Liu and X. Wang, "Plant diseases and pests detection based on deep learning: A review," *Plant Methods*, vol. 17, no. 1, p. 22, Dec. 2021, doi: 10.1186/s13007-021-00722-9.

[10] D. P. Hughes and M. Salathe, "An open access repository of images on plant health to enable the development of mobile disease diagnostics," 2015, *arXiv:1511.08060*.

[11] M. Fawakherji, C. Potena, A. Pretto, D. D. Bloisi, and D. Nardi, "Multi-spectral image synthesis for crop/weed segmentation in precision farming," *Robot. Auto. Syst.*, vol. 146, Dec. 2021, Art. no. 103861, doi: 10.1016/j.robot.2021.103861.

[12] M. Minervini, A. Fischbach, H. Scharr, and S. A. Tsaftaris, "Finely-grained annotated datasets for image-based plant phenotyping," *Pattern Recognit. Lett.*, vol. 81, pp. 80–89, Oct. 2016, doi: 10.1016/j.patrec.2015.10.013.

[13] J. Chen, J. Chen, D. Zhang, Y. Sun, and Y. A. Nanehkaran, "Using deep transfer learning for image-based plant disease identification," *Comput. Electron. Agricult.*, vol. 173, Jun. 2020, Art. no. 105393, doi: 10.1016/j.compag.2020.105393.

[14] V. Binnar and S. Sharma, "Plant leaf diseases detection using deep learning algorithms," in *Machine Learning, Image Processing, Network Security and Data Sciences* (Lecture Notes in Electrical Engineering), vol. 946, R. Doriya, B. Soni, A. Shukla, and X. Z. Gao, Eds. Singapore: Springer, 2023, pp. 217–228, doi: 10.1007/978-981-19-5868-7_17.

[15] J. Andrew, J. Eunice, D. E. Popescu, M. K. Chowdary, and J. Hemanth, "Deep learning-based leaf disease detection in crops using images for agricultural applications," *Agronomy*, vol. 12, no. 10, p. 2395, Oct. 2022, doi: 10.3390/agronomy12102395.

[16] Ü. Atila, M. Uçar, K. Akyol, and E. Uçar, "Plant leaf disease classification using EfficientNet deep learning model," *Ecological Informat.*, vol. 61, Mar. 2021, Art. no. 101182, doi: 10.1016/j.ecoinf.2020.101182.

[17] M. Gehlot and G. C. Gandhi, "'EffiNet-TS': A deep interpretable architecture using EfficientNet for plant disease detection and visualization," *J. Plant Diseases Protection*, vol. 130, no. 2, pp. 413–430, Apr. 2023, doi: 10.1007/s41348-023-00707-x.

[18] P. Sharma, Y. P. S. Berwal, and W. Ghai, "Performance analysis of deep learning CNN models for disease detection in plants using image segmentation," *Inf. Process. Agricult.*, vol. 7, no. 4, pp. 566–574, Dec. 2020, doi: 10.1016/j.inpa.2019.11.001.

[19] A. Haridasan, J. Thomas, and E. D. Raj, "Deep learning system for paddy plant disease detection and classification," *Environ. Monit. Assessment*, vol. 195, Jan. 2023, Art. no. 120, doi: 10.1007/s10661-022-10656-x.

[20] Y. Kaya and E. Gürsoy, "A novel multi-head CNN design to identify plant diseases using the fusion of RGB images," *Ecological Informat.*, vol. 75, Jul. 2023, Art. no. 101998, doi: 10.1016/j.ecoinf.2023.101998.

[21] J. D. Stamford, S. Vialet-Chabrand, I. Cameron, and T. Lawson, "Development of an accurate low cost NDVI imaging system for assessing plant health," *Plant Methods*, vol. 19, no. 1, Jan. 2023, Art. no. 9, doi: 10.1186/s13007-023-00981-8.

[22] S. Puteh, N. F. M. Rodzali, A. P. P. A. Majeed, I. M. Khairuddin, Z. Z. Ibrahim, and M. A. M. Razman, "Classification of *Capsicum frutescens* health condition through features extraction from NDVI values using image processing," in *RiTA 2020* (Lecture Notes in Mechanical Engineering). Singapore: Springer, 2021, pp. 414–423, doi: 10.1007/978-981-16-4803-8_41.

[23] H. M. Sahin, T. Miftahushudur, B. Grieve, and H. Yin, "Segmentation of weeds and crops using multispectral imaging and CRF-enhanced U-Net," *Comput. Electron. Agricult.*, vol. 211, Aug. 2023, Art. no. 107956, doi: 10.1016/j.compag.2023.107956.

[24] L. Costa, L. Nunes, and Y. Ampatzidis, "A new visible band index (vNDVI) for estimating NDVI values on RGB images utilizing genetic algorithms," *Comput. Electron. Agricult.*, vol. 172, May 2020, Art. no. 105334, doi: 10.1016/j.compag.2020.105334.

[25] J. Yue, J. Tian, W. Philpot, Q. Tian, H. Feng, and Y. Fu, "VNAI-NDVI-space and polar coordinate method for assessing crop leaf chlorophyll content and fractional cover," *Comput. Electron. Agricult.*, vol. 207, Apr. 2023, Art. no. 107758, doi: 10.1016/j.compag.2023.107758.

[26] A. Voitik, V. Kravchenko, O. Pushka, T. Kutkovetska, T. Shchur, and S. Kocira, "Comparison of NDVI, NDRE, MSAVI and NDSI indices for early diagnosis of crop problems," *Agricult. Eng.*, vol. 27, no. 1, pp. 47–57, Jan. 2023, doi: 10.2478/agriceng-2023-0004.

[27] Y. Lu, K. Xu, L. Zhang, M. Deguchi, H. Shishido, T. Arie, R. Pan, A. Hayashi, L. Shen, S. Akita, and K. Takei, "Multimodal plant healthcare flexible sensor system," *ACS Nano*, vol. 14, no. 9, pp. 10966–10975, Sep. 2020, doi: 10.1021/acsnano.0c03757.

[28] H. Wu, R. Nißler, V. Morris, N. Herrmann, P. Hu, S.-J. Jeon, S. Kruss, and J. P. Giraldo, "Monitoring plant health with near-infrared fluorescent H_2O^2 nanosensors," *Nano Lett.*, vol. 20, no. 4, pp. 2432–2442, Apr. 2020, doi: 10.1021/acs.nanolett.9b05159.

[29] N. Carion, F. Massa, G. Synnaeve, N. Usunier, A. Kirillov, and S. Zagoruyko, "End-to-end object detection with transformers," 2020, *2005.12872*.

[30] H. Zhang, F. Li, S. Liu, L. Zhang, H. Su, J. Zhu, L. M. Ni, and H.-Y. Shum, "DINO: DETR with improved DeNoising anchor boxes for end-to-end object detection," 2022, *arXiv:2203.03605*.

[31] K. He, X. Chen, S. Xie, Y. Li, P. Dollár, and R. Girshick, "Masked autoencoders are scalable vision learners," 2021, *arXiv:2111.06377*.

[32] A. Radford, J. W. Kim, C. Hallacy, A. Ramesh, G. Goh, S. Agarwal, G. Sastry, A. Askell, P. Mishkin, J. Clark, G. Krueger, and I. Sutskever, "Learning transferable visual models from natural language supervision," 2021, *arXiv:2103.00020*.
[33] P. J. Sellers, "Canopy reflectance, photosynthesis, and transpiration, II. The role of biophysics in the linearity of their interdependence," *Remote Sens. Environ.*, vol. 21, no. 2, pp. 143–183, Mar. 1987, doi: 10.1016/0034-4257(87)90051-4.
[34] J. W. Rouse Jr., R. H. Haas, J. A. Schell, and D. W. Deering. (1973). *Monitoring the Vernal Advancement and Retrogradation (green Wave Effect) of Natural Vegetation*. [Online]. Available: https://ntrs.nasa.gov/api/citations/19750020419/downloads/19750020419.pdf
[35] A. A. Gitelson, Y. J. Kaufman, and D. Rundquist, "Novel algorithms for remote estimation of vegetation fraction," *Remote Sens. Environ.*, vol. 80, no. 1, pp. 76–87, 2002, doi: 10.1016/S0034-4257.
[36] N. Ohta and A. R. Robertson, "CIE standard colourimetric system," in *Colorimetry: Fundamentals and Applications*. USA: Wiley, 2005, doi: 10.1002/0470094745.ch3.
[37] J. Schanda, "3 CIE colourimetry," in *Colorimetry: Understanding the CIE System*, J. Schanda, Ed. Hoboken, NJ, USA: Wiley, 2007, p. 74.
[38] K. L. Kelly, "Lines of constant correlated color temperature based on MacAdam's (μ,ν) uniform chromaticity transformation of the CIE diagram," *J. Opt. Soc. Amer.*, vol. 53, no. 8, p. 999, Aug. 1963, doi: 10.1364/josa.53.000999.
[39] A. K. Khaple, G. M. Devagiri, N. Veerabhadraswamy, S. Babu, and S. B. Mishra, "Vegetation biomass and carbon stock assessment using geospatial approach," in *Forest Resources Resilience and Conflicts*. The Netherlands: Elsevier, 2021, pp. 77–91, doi: 10.1016/B978-0-12-822931-6.00006-X.
[40] *LNDVI*. Accessed: May 31, 2023. [Online]. Availabile: https://github.com/codex-exe/LNDVI
[41] *FAOSTAT*. Accessed: May 31, 2023. [Online]. Availabile: https://www.fao.org/faostat/en/#data/RP/visualize
[42] S. S. Chouhan, U. P. Singh, and S. Jain, "Applications of computer vision in plant pathology: A survey," *Arch. Comput. Methods Eng.*, vol. 27, no. 2, pp. 611–632, Apr. 2020.
[43] Y. A. Nanehkaran, D. Zhang, J. Chen, Y. Tian, and N. Al-Nabhan, "Recognition of plant leaf diseases based on computer vision," *J. Ambient Intell. Humanized Comput.*, vol. 2020, pp. 1–18, Sep. 2020.

ANANTHAKRISHNAN BALASUNDARAM (Member, IEEE) received the master's degree in computer science and engineering from B. S. Abdur Rahman University, Chennai, India, and the Doctor of Philosophy (Ph.D.) degree in computer science and engineering from Anna University, India. He is currently an Associate Professor with the School of Computer Science and Engineering and also associated with the Research Center for Cyber Physical Systems, Vellore Institute of Technology (VIT)—Chennai Campus. He has an overall experience of 14 years of which he has over nine years of industrial experience working across MNCs like Cognizant Technology Solutions (CTS), Tata Consultancy Services (TCS), and iGATE Global Solutions and five years of academic experience. His research interests include deep neural networks, computer vision, video analytics, image and video processing, artificial intelligence, data warehousing, and data mining. His current research interests include healthcare intelligence, medical image analysis, and smart agriculture. He has received five best paper awards so far across international conferences. He has also received the Star Performer Award at Cognizant Technology Solutions and Quality and Delivery Excellence Award at iGATE Global Solutions. He is also an active reviewer for reputed international SCIE journals of Elsevier, IEEE, and Springer. He has also served as a guest editor for special issues in a couple of SCI journals.

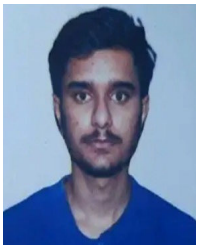

ALABHYA SHARMA was born in Himachal Pradesh, India, in 2003. He is currently pursuing the Bachelor of Technology degree in computer science and engineering with specialization in artificial international and robotics with Vellore Institute of Technology (VIT), Chennai. In May 2023, he did a research internship from the Center for Cyber Physical Systems, VIT Chennai, wherein his research interests include precision agriculture, computer vision, artificial intelligence, robotics perception, deep learning, and reinforcement learning.

SWAATHY KUMARAVELAN is currently pursuing the Graduate degree with Vellore Institute of Technology, Chennai. Her research interests include cloud technology, software development, and artificial intelligence. She is passionate about solving real world problems and building products. Outside academics and technology, she is constantly striving to be a better classical dancer (Bharatanatyam).

AYESHA SHAIK (Member, IEEE) received the Doctor of Philosophy (Ph.D.) degree from IIITDM Kanchipuram. She is currently a Senior Assistant Professor with the School of Computer Science and Engineering and also associated with the Research Center for Cyber Physical Systems, Vellore Institute of Technology (VIT)—Chennai Campus. Her research interests include image processing, digital image processing, watermarking, and deep learning.

MUTHU SUBASH KAVITHA received the Ph.D. degree in information engineering from Hiroshima University, Japan, in 2012. Since then, she has held various positions in academia. Since 2012, she has been a Postdoctoral Fellow with Seoul National University. Following that, she was a Research Professor with Kyungpook National University, South Korea, until 2018. She was honored as a JSPS International Research Fellow and held the position of a specially appointed Assistant Professor with the Graduate School of Advanced Science and Engineering, Hiroshima University, until 2021. Currently, she is an Assistant Professor with the School of Information and Data Sciences, Nagasaki University. Her research interests include image processing algorithms for image pattern analysis, machine learning, artificial intelligence, pattern recognition, and deep learning techniques.